

Generic features of the spectrum of trapped polarized fermions

Erich J. Mueller

Laboratory of Atomic and Solid State Physics, Cornell University, Ithaca NY 14853

(Dated: August 18, 2008)

We show that bimodal radio frequency spectra universally arise at intermediate temperatures in models of strongly interacting trapped Fermi gases. The bimodality is independent of superfluidity or pseudogap physics, depending only on the functional form of the equation of state – which is constrained by dimensional analysis at low temperatures and the virial expansion at high temperatures. In addition to these model independent results, we present a simple calculation of the radio frequency line-shape of a highly polarized Fermi gas which uses energetic considerations to include final state interactions. While this model only qualitatively captures the line-shapes observed in the experiments, it provides a conceptually clean and powerful technique for estimating the energy scales and how they vary with experimental parameters.

PACS numbers: 03.75.Ss, 05.30.Fk

Can spectroscopy be used to detect pairing in a gas of fermionic atoms? The paradigm for thinking about this question was set in 2003, when Greiner, Regal and Jin [1] presented an experimental study of the microwave spectrum of a two component gas of ^{40}K on the BEC side of resonance (where two potassium atoms are capable of forming weakly bound molecules). Their sample consisted of a noncondensed gas of diatomic molecules in chemical equilibrium with a gas of atoms. They found an easily interpreted bimodal spectrum: a sharp line came from the excitations of free atoms, and a broad peak from the dissociation of molecules. Later experiments on colder samples in different parameter ranges showed similar bimodality and were interpreted in similar ways [2, 3]. In particular, when such a bimodal peak was seen by Chin, Bartensein, Altmeyer, Riedl, Jochim, Denschlag, and Grimm [2] on the BCS side of resonance, it was taken as a sign of Cooper pairing. This interpretation was further reinforced by mean field calculations which showed that the finite temperature trapped paired gas does indeed produce bimodal spectra [4, 5, 6, 7]. This paradigm has been shattered by the realization that there exist models which produce bimodal spectra in the absence of pairing [8]. Here we give a simple argument for why trapped strongly interacting Fermi gases *generically* show a bimodal spectrum, irrespective of the presence of pairing.

Our argument relies on two ingredients: a harmonic trap plus qualitative features of the equation of state. We establish that the equation of state of the unitary Fermi gas has these features through a dimensional analysis argument supplemented by the first terms of the virial expansion. Consistent with previous results [4, 5, 6, 7, 8], we conclude that one of the spectral peaks comes from atoms at the edge of the cloud, and the other from atoms at the center. This is similar to the mechanism by which multiple spectral peaks appear in the spectra of clouds of Bosons in an optical lattice [9, 10].

We quantify our arguments by presenting a simplified

calculation of the spectrum of a trapped two-component Fermi gas in the limit $n_{\downarrow}/n_{\uparrow} \rightarrow 0$. Although we include final-state interactions [11, 12, 13, 14, 15, 16, 17, 18, 19] in our quantitative calculations, we emphasize that the bimodality is *not* a final-state effect. In the highly polarized limit, final state effects set the frequency scale for the spectral line but do not significantly change its shape or temperature dependence. Moving away from this limit of large polarizations, final state interactions can have more profound effects [11, 12, 13, 14, 15, 16, 17, 18, 19, 20, 21, 22].

We consider an experiment on a gas of atoms with two spin state: \uparrow and \downarrow . We imagine that a probe (for example radio waves) excites atoms from the \downarrow state to a third state x . In most recent experiments on ^6Li the states involved are the three lowest energy hyperfine states $|\uparrow\rangle = |1\rangle$, $|\downarrow\rangle = |2\rangle$ and $|x\rangle = |3\rangle$, ($E_1 < E_2 < E_3$) though other combinations are possible [22]. The spectrum $I(\nu)$ measures, for a fixed probe intensity, the rate of population transfer from \downarrow to x as a function of the detuning ν from the free-space resonance.

In principle, moments of this spectrum can be calculated from the sum rule [11, 12, 13], $\bar{\nu} = \int d\nu \nu I(\nu) / \int d\nu I(\nu) = \frac{1}{n_{\downarrow}} \int d^3r [v_{\uparrow x}(r) - v_{\uparrow \downarrow}(r)] \langle \psi_{\uparrow}^{\dagger}(r) \psi_{\downarrow}^{\dagger}(0) \psi_{\downarrow}(0) \psi_{\uparrow}(r) \rangle$, where $v_{ij}(r)$ is the interaction potential between atoms in states i and j , and ψ_{σ} is an annihilation operator. As pointed out by Pethick and Stoof [23], extracting useful information from this result is problematic because this expectation value (which is closely related to the expectation value of the interaction energy) is not a low energy observable: different potentials which give rise to the same low energy scattering properties will give completely different values for $\bar{\nu}$; hard spheres have $\bar{\nu} = 0$, while point interaction yield $\bar{\nu} = \infty$. These potential dependent features come from the largely unobservable ultraviolet tail of the spectrum. The peak of the spectral line occurs at relatively small ν and only depends on low energy properties such as the scattering lengths a_{ij} .

Here, we explicitly restrict our discussion to the peak of this extended spectrum, beginning with the conceptually simple limit where there is a single down-spin particle in a gas of up-spin particles with *uniform* density n_\uparrow . Barring pathologies in the matrix elements of the probe, and subtleties associated with vertex corrections [23], the peak in $I(\nu)$ should be located at detuning

$$\nu_p(n_\uparrow) = \epsilon_x(n_\uparrow) - \epsilon_\downarrow(n_\uparrow), \quad (1)$$

where $\epsilon_\sigma(n_\uparrow)$ is the energy of a single particle of spin σ in the sea of \uparrow atoms. Note that ϵ_σ is neither the self-energy, nor the chemical potential, though it can be derived from the self-energy by integrating with respect to the coupling constant [24]. The fact that $\epsilon_\sigma \neq \mu_\sigma$ is clear from considering the dilute high temperature limit, where μ_σ is very negative, but ϵ_σ is very small. Assuming that the inhomogeneous broadening dominates the lineshape, one can approximate the homogeneous lineshape as a delta function. In a trapped gas, applying this approximation locally will yield an inhomogeneous spectrum

$$I(\nu) \propto \int d^3r n_\downarrow(r) \delta(\nu - \nu_p(n_\uparrow(r))). \quad (2)$$

Note that we are explicitly neglecting the role of “Frank-Condon” factors, related to overlaps between the states in the two channels, and do not include “excitonic” effects related to pairing in the final state [15, 16, 17, 18, 19]. To correctly model the uniform spectrum, as experimentally studied in [21, 22], it would be essential to include such factors.

Given that n_\downarrow is vanishingly small, and that for short-range interactions atoms in the \uparrow state will not interact with one-another, we take $n_\uparrow(r)$ to be given by the standard non-interacting result.

$$n_\uparrow(r) = -\frac{1}{\lambda_T^3} g_{3/2}(-e^{\beta(\mu_\uparrow - V(r))}) \quad (3)$$

where we have used the Thomas-Fermi approximation to account for the slowly varying trap potential $V(r)$. For harmonic traps, this Thomas-Fermi approximation is excellent, even at zero temperature and for small numbers of particles [25]. The density is expressed in terms of the polylogarithm function $g_{3/2}(z) = \sum_j z^j / j^{3/2}$ and the thermal wavelength $\lambda_T^2 = 2\pi\hbar^2 / mk_B T$. Similarly the down-spin density is

$$n_\downarrow(r) = \frac{1}{\lambda_T^3} e^{\beta[\mu_\downarrow - V(r) - \epsilon_\downarrow(n_\uparrow(r))]} \quad (4)$$

where we have assumed $\mu_\downarrow < 0$ and $|\beta\mu_\downarrow| \gg 1$. Defining the function $\mu(\nu)$ to be the inverse of ν_p , *i.e.* $\nu_p[\mu(\nu)] = \nu$, and assuming a harmonic trap: $V(r) \propto r^2$, the spectrum is

$$I(\nu) \propto \sqrt{\mu_\uparrow^{(0)} - \mu(\nu)} e^{-\beta\epsilon_\downarrow[\mu(\nu)]} \frac{\partial}{\partial \nu} e^{\beta\mu(\nu)}. \quad (5)$$

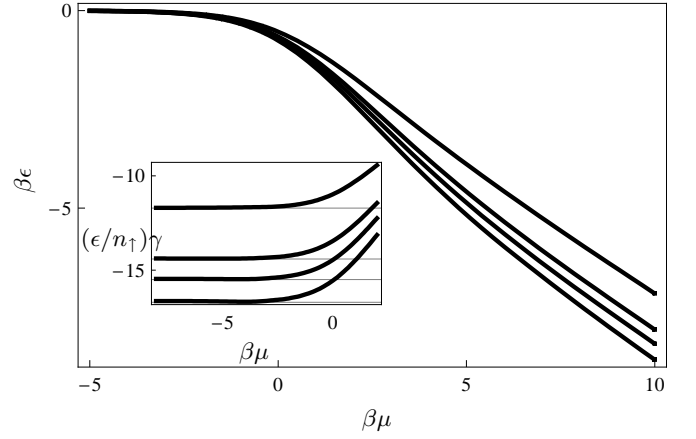


FIG. 1: Energy of a single minority species atom in a Fermi sea of majority species calculated from Nozieres and Schmidt Rink free energy. Inset shows energy scaled by majority species density n_\uparrow and the factor $\gamma = (k_B T)^{1/2} (m/\hbar^2)^{3/2}$ – horizontal lines correspond to leading order virial expansion. From bottom to top $a\sqrt{mk_B T/\hbar^2} = \infty, -10, -5, -2$.

We now argue that for short range interactions, $\epsilon_\sigma(\mu_\uparrow)$ must have the generic form illustrated in figure 1. By considering a virial expansion, we know that for $\beta\mu_\uparrow$ sufficiently negative, ϵ must be proportional to n_\uparrow [26], and hence will be exponentially small in $\beta\mu_\uparrow$. For sufficiently large $\beta\mu_\uparrow$, the scattering will be unitarity limited and ϵ will be linear in $\beta\mu_\uparrow$. Different theories can only change the slope of the latter relationship, and change the exact location of the crossover between these two limiting behaviors. Regardless of these two details, the resulting inhomogeneously broadened spectrum will have the following features: (i) At all temperatures, the edge of the cloud will contribute spectral weight at $\nu = 0$: for a harmonic trap a weak $\sqrt{-\log(\beta\nu)}$ divergence will be found. (ii) At high temperatures ($\beta\mu_\uparrow < 0, |\beta\mu_\uparrow| \gg 1$), all spectral weight will be in this peak. Including additional sources of broadening will obscure the singularity, yielding simply an asymmetric peak. (iii) At very low temperatures ($\beta\mu \gg 1$) only an exponentially small fraction of the spectral weight will be in this low detuning peak, and it will not be observable. Rather, most of the spectral weight will come from the center of the cloud where most of the down-spin particles reside. This will give a single broad peak. At sufficiently high central density ($n_\uparrow a^3 \gg 1$), the location of this peak will scale linearly with the central up-spin chemical potential. The constant of proportionality will depend on final-state interactions. (iv) At intermediate temperatures a bimodal structure will be seen. Illustrative spectra are shown in figure 2. It should be clear that our interpretation of the spectra is vastly different from the canonical one [2, 3], where the two peaks are attributed to “atoms” and “pairs”.

Although the qualitative spectral features are generic,

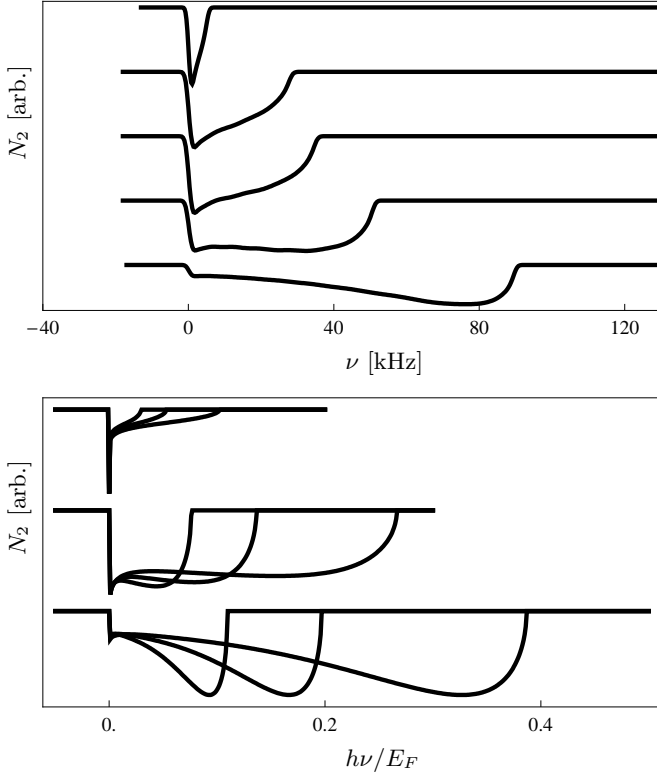


FIG. 2: Radio frequency spectra of a harmonically trapped gas in the limit of vanishing N_2 : number of atoms remaining in the 2 state as a function of the detuning ν of the probe from the vacuum transition value (offset vertically for clarity). In all cases $a_{12} = \infty$. Top figure measures frequencies in physical units for experimentally relevant parameters: from top to bottom $a_{13}\sqrt{mk_B T/\hbar^2} = -3, -2.6, -2.4, -2.4, -1.8$ with $T/T_F = 1.9, 1, 0.9, 0.7, 0.5$ and $E_f = k_B T_F = 260\text{hkHz}, 360\text{hkHz}, 360\text{hkHz}, 360\text{hkHz}$, where $E_f = (3N\omega_x\omega_y\omega_z)^{1/3}/\pi$ measures the number of majority species atoms, with ω_j the small oscillation frequency in direction j , and h is Planck's constant. Lower figure measures frequencies in units of E_f : From top to bottom $T/T_f = 1.25, 0.7, 0.5$, while from left to right $a\sqrt{mk_B T/\hbar^2} = -5, -2.55, -1$. The shape of the spectrum is mainly set by T/T_f , while the frequency scale depends on the interaction strength. The upper figures are convolved with a Gaussian of width $0.003E_f$, while no broadening is used in the lower figures.

we make quantitative predictions by calculating the energies in figure 1 from the generalization of the Noziers and Schmitt-Rink free energy [27] to unequal densities. Within this approximation, which can be thought of as pairwise summing all scattering events, taking into account medium effects by a phase space reduction factor, the interaction contribution to the free energy is

$$\delta\Omega = -\pi \int \frac{d^3k}{(2\pi)^3} \int \frac{d\omega}{2\pi} g(\omega) \arg\left(\frac{1}{4\pi a} + \theta(k, \omega)\right) \quad (6)$$

$$\theta(k, \omega) = \int \frac{d^3q}{(2\pi)^3} \left[\frac{1 - f_{q-k/2}^\uparrow - f_{q+k/2}^\downarrow}{\omega - q^2/m - k^2/4m} + \frac{m}{q^2} \right],$$

where the inverse temperature β enters in the Bose

and Fermi functions $g(\omega) = (e^{\beta\omega} - 1)^{-1}$, $f_k^\sigma = (e^{\beta(k^2/2m - \mu_\sigma)} - 1)^{-1}$. Replacing \downarrow with x (and using the appropriate scattering length) gives the equivalent quantity in the excited state. As in the standard derivation of the Gibbs-Duhem relation, dimensional analysis requires that the free energy density is of the form $\beta\Omega/V = \lambda^{-3}f(a/\lambda, \beta\mu_\uparrow, \beta\mu_\downarrow)$. Since in the limit of low down-spin density this will be proportional to the number of down-spins, we have that the interaction energy will be of the form $N_\downarrow\epsilon_\downarrow = E_{\text{int}} = \Omega - \Omega_0 - TS - \mu_\uparrow N_\uparrow - \mu_\downarrow = (-3/2)\delta\Omega - (1/2)a\partial\delta\Omega/\partial a$. As one tunes from the dilute limit, $na^3 \ll 1$, to unitarity, the interaction energy goes from $E_{\text{int}} = -2\delta\Omega$ to $E_{\text{int}} = -3/2\delta\Omega$ [28]. Formally one can write Eq. (6) in the limit $\beta\mu \rightarrow -\infty$,

$$\frac{\delta\Omega}{N_\downarrow} \Big|_{N_\downarrow=0} = 2\lambda_T^3 \int_0^\infty dq \int_0^\infty d\nu q^2 e^{-\beta(\nu + \frac{q^2}{4m} - \mu_\uparrow)} \times \arg\left(\frac{1}{4\pi a} + \theta\right). \quad (7)$$

Where θ , defined in Eq. (6), is evaluated with $f^\downarrow = 0$, implying it is only a function of $\nu = \omega + \mu_\uparrow + \mu_\downarrow - q^2/4m, \beta, q$ and μ_\uparrow . At low temperature, $\beta\mu_\uparrow \gg 1$, this integral is poorly behaved and is best replaced by a low temperature expansion whose leading term is

$$\frac{\delta\Omega}{N_\downarrow} \Big|_{T, N_\downarrow=0} = \frac{1}{(2\pi)^2} \frac{\hbar^2}{m} \int_0^\infty \frac{q^2 dq}{(4\pi a)^{-1} + \text{Re}(\theta)}, \quad (8)$$

where θ can be calculated analytically, and is evaluated at $\nu = q^2/4m$. At unitarity we find $\epsilon = -0.69\mu_\uparrow$, a reasonable approximation to the results of quantum Monte-Carlo [29]. Given that the lowest temperature highly polarized data from [3] has $\beta\mu_\uparrow = 1.25$, finite temperature effects are crucial and the asymptotic result cannot be compared to experiment.

As previously anticipated, at high temperatures Eq. (7) reduces to the polarization-imbalanced virial expansion result $\epsilon = \sqrt{2}k_B T \lambda_T^3 n_\uparrow (-3b_2/4 - y\partial b_2/\partial y)$ (cf. [28]), where the second virial coefficient is $b_2 = (1/\pi) \int_0^\infty dx/(1+x^2)e^{-x^2/y}$, with $y = mk_B T a^2/\hbar^2$. At low densities ($na^3 \ll 1$) we can analytically integrate (6) to recover $\epsilon = (4\pi\hbar^2/m)an_\uparrow$, regardless of temperature.

The spectra in figure 2 capture many features of the experiments [3] and of more numerically demanding theories [7, 8]. The most successful element is that since we include final state interactions we are able to reproduce the energy scales observed in experiment. Additionally, as already emphasized, our intermediate temperature spectra are bimodal – however the bimodality is much much less pronounced in our theory than in the experiment. By comparing with the calculation of Massignan, Bruun, and Stoof [8], we can understand this discrepancy as an artifact of neglecting the width of the homogeneous spectrum – due in part to the fact that at higher densities the initial $|\downarrow\rangle$ state has overlap with many $|x\rangle$ states. The intermediate detuning spectral weight (for example around 10 kHz in figure 2) will be

reduced by this broadening, more clearly separating the spectrum into two peaks. In experiments, finite probe duration further broadens the spectrum, and the finite probe size and trap anharmonicities distort the low detuning peak.

Having understood the case $n_{\downarrow}/n_{\uparrow} \ll 1$, we now address the balanced situation $n_{\downarrow} = n_{\uparrow}$. It should be clear that all of our arguments about the scaling of the energy with density carry over to the unpolarized gas. Thus, to the extent that the homogeneous spectrum consists of a single peak, one expects that the trapped spectra should have the same qualitative features that we saw in figure 2. Indeed, there is very little qualitative difference between the experimental spectra of polarized and unpolarized atoms in a trap [3].

On the other hand, our quantitative calculations do not generalize easily to the unpolarized case. The physics of the unpolarized gas is more complicated than that of the highly polarized gas: with increasing n_{\downarrow} the down-spin atoms occupy a larger range of momentum states, the up-spin Fermi sea becomes increasingly perturbed, and the normal state eventually becomes unstable to forming a superfluid. While RF spectroscopy is undoubtedly sensitive to these many-body effects, their manifestation may be subtle, sensitive to final state interactions, and easily obscured by the trap inhomogeneities. There does not appear to be a model independent way to use inhomogeneously broadened spectra to demonstrate superfluidity or extract a pairing gap.

Finally, we mention that with minor changes our qualitative arguments also apply in the simpler case of a weakly interacting Bose gas, such as spin polarized hydrogen [30]. In these gases the interaction energy is proportional to the density. At low temperature, $n\lambda_T^3 > 1$, the density is proportional to the chemical potential, while at high temperature, $n\lambda_T^3 \ll 1$, the density is exponentially small in $\beta\mu$. Following the arguments presented here, one will therefore see a bimodal spectrum in a trapped Bose gas at intermediate temperatures. Such bimodality is indeed found [31].

I would like to thank Sourish Basu, Francesco Fumarola, Kaden Hazzard, Tin-Lun Ho, Wolfgang Ketterle, Kathy Levin, Mohit Randeria, Henk Stoof, Paivi Torma, and W. Zwerger for various discussions and critical comments about this work. This work was supported in part by the National Science Foundation through grants PHY-0456261 and PHY-0758104.

[1] M. Greiner, C.A. Regal, and D.S. Jin, Phys. Rev. Lett. **94**, 070403 (2005).

[2] C. Chin, M. Bartenstein, A. Altmeyer, S. Riedl, S. Jochim, J. H. Denschlag, and R. Grimm, Science **305**, 1128 (2004).

[3] C. H. Schunck, Y. Shin, A. Schirotzek, M. W. Zwierlein, and W. Ketterle, Science **316**, 867 (2007).

[4] J. Kinnunen, M. Rodriguez, and P. Törmä, Science **305**, 1131 (2004).

[5] Y. Ohashi and A. Griffin, Phys. Rev. A **72**, 013601 (2005).

[6] Yan He, Qijin Chen, and K. Levin, Phys. Rev. A **72**, 011602(R) (2005).

[7] Yan He, Chih-Chun Chien, Qijin Chen, and K. Levin, Phys. Rev. A **77**, 011602(R) (2008).

[8] P. Massignan, G. M. Bruun, and H. T. C. Stoof, Phys. Rev. A **77**, 031601(R) (2008).

[9] Gretchen K. Campbell, Jongchul Mun, Micah Boyd, Patrick Medley, Aaron E. Leanhardt, Luis G. Marcassa, David E. Pritchard, Wolfgang Ketterle, Science **313**, 649 (2006).

[10] Kaden R.A. Hazzard, and Erich J. Mueller, Phys. Rev. A **76**, 063612 (2007).

[11] M. Punk and W. Zwerger, arXiv:0707.0792 (2007).

[12] Z. Yu and G. Baym, Phys. Rev. A **73**, 063601 (2006).

[13] G. Baym, C. J. Pethick, Z. Yu, and M.W. Zwierlein, arXiv:0707.0859.

[14] C. Chin and P.S. Julienne, Phys. Rev. A **71**, 012713 (2005).

[15] A. Perali, P. Pieri, G.C. Strinati, arXiv:0709.0817 (2007).

[16] Yan He, Chih-Chun Chien, Qijin Chen, and K. Levin arXiv:0804.1429 (2008).

[17] P. Massignan, G. M. Bruun, and H. T. C. Stoof arXiv:0805.3667 (2008).

[18] Martin Veillette, Eun Gook Moon, Austen Lamacraft, Leo Radzihovsky, Subir Sachdev, D.E. Sheehy arXiv:0803.2517 (2008).

[19] Sourish Basu and Erich J. Mueller, Phys. Rev. Lett. **101**, 060405 (2008).

[20] S. Gupta et al. Science **300**, 475 (2003); M.W. Zwierlein et al. Phys. Rev. Lett. **91**, 250404 (2003).

[21] Y. Shin, C.H. Schunck, A. Schirotzek, and W. Ketterle, Phys. Rev. Lett. **99**, 090403 (2007).

[22] Christian H. Schunck, Yong-il Shin, Andre Schirotzek, Wolfgang Ketterle, Nature **454**, 739-743 (2008).

[23] C. J. Pethick and H. T. C. Stoof, Phys. Rev. A **64**, 013618 (2001).

[24] Gerald D. Mahan, "Many Particle Physics", Plenum Press (New York, 1990), chap.4.1.

[25] Erich J. Mueller, Phys. Rev. Lett. **93**, 190404 (2004).

[26] Tin-Lun Ho, and Erich J Mueller, Phys. Rev. Lett. **92**, 160404 (2004).

[27] P. Nozières and S. Schmitt-Rink, J. Low Temp. Phys. **59**, 195 (1985).

[28] Tin-Lun Ho, Phys. Rev. Lett. **92**, 090402 (2004).

[29] C. Lobo, A. Recati, S. Giorgini, and S. Stringari, Phys. Rev. Lett. **97**, 200403 (2006).

[30] Kaden R.A. Hazzard, private communications.

[31] Dale G. Fried, Thomas C. Killian, Lorenz Willmann, David Landhuis, Stephen C. Moss, Daniel Kleppner, and Thomas J. Greytak, Phys. Rev. Lett. **81**, 3811 (1998).